



## Search for Direct Pair Production of Scalar Top Quark in $p\bar{p}$ Collisions at $\sqrt{s} = 1.96$ TeV

The CDF Collaboration  
URL <http://www-cdf.fnal.gov>  
(Dated: January 30, 2005)

We have searched for direct pair production of scalar top quarks using  $163 \text{ pb}^{-1}$  of proton-antiproton collision data recorded by the CDF experiment during Run II of the Tevatron. The scalar top quarks are sought via their decay into a charm quark and a neutralino, which is assumed to be the lightest supersymmetric particle. The event signature is missing transverse energy and several high- $E_T$  jets. In the scalar top quark signal region, 11 events are observed with  $8.3_{-1.7}^{+2.3}$  expected from Standard Model processes. Thus no evidence for scalar top quark is observed, and 95% CL. limits are set on the cross section times squared branching ratio as function of the scalar top quark mass, for several neutralino masses. We assume 100% branching ratio for scalar top quark decays into charm quark and neutralino.

*Preliminary Results for Winter 2005 Conferences*

## I. INTRODUCTION

Supersymmetry (SUSY) [1] is one of the most popular extensions to the Standard Model (SM) of particle physics. It overcomes some of the theoretical problems in the SM by introducing new degrees of freedom. In this model a scalar supersymmetric partner is assigned to every SM fermion, and a fermionic superpartner to every SM boson. Therefore the SM quark helicity states  $q_L$  and  $q_R$  acquire scalar partners  $\tilde{q}_L$  and  $\tilde{q}_R$ . The mass eigenstates of each scalar quark is a mixture of its weak eigenstates. The amount of splitting of the mass eigenvalues depends on the mass and the Yukawa coupling of its SM partner. Due to the large top quark mass and the large value of its Yukawa coupling constant (Higgs-to-top coupling), there is a significant split in the mass between the two mass eigenstates  $\tilde{t}_1$  and  $\tilde{t}_2$ . Thus it is likely that the lighter scalar top ( $\tilde{t}_1$ ) may be the lightest squark, and it can be even lighter than the top quark. From here on the stop quark that is discussed in the paper is the lighter mass eigenstate  $\tilde{t}_1$ .

At the Tevatron, the scalar top quarks are expected to be produced in pairs via  $gg$  fusion and  $q\bar{q}$  annihilation. In this analysis, the scalar top quark is searched in the channel  $p\bar{p} \rightarrow \tilde{t}_1\bar{\tilde{t}}_1 \rightarrow (c\tilde{\chi}_1^0)(\bar{c}\tilde{\chi}_1^0)$ . The lightest neutralino  $\tilde{\chi}_1^0$  is assumed to be the lightest supersymmetric particle and stable. This leads to experimental signatures with appreciable missing transverse energy. The decay  $\tilde{t}_1 \rightarrow c\tilde{\chi}_1^0$  dominates via a one-loop diagram in the absence of flavor-changing neutral currents if  $m_{\tilde{t}_1} < m_b + m_{\chi_1^\pm}$ ,  $m_{\tilde{t}_1} < m_W + m_b + m_{\chi_1^0}$ ,  $m_{\tilde{t}_1} < m_b + m_{\tilde{\nu}}$ , and  $m_{\tilde{t}_1} < m_b + m_{\tilde{\tau}}$ . The signature of the process in this search is a pair of acolinear heavy flavor jets in the transverse plane, large  $\cancel{E}_T$ , and no isolated high  $p_T$  leptons in the final state. In Run I this channel of stop search had been performed by CDF [2] and DØ [3]. CDF (DØ) excluded stop mass below  $m_{\tilde{t}_1} = 119$  GeV/ $c^2$  ( $m_{\tilde{t}_1} = 122$  GeV/ $c^2$ ) for  $m_{\tilde{\chi}_1^0} = 40$  GeV/ $c^2$  ( $m_{\tilde{\chi}_1^0} = 45$  GeV/ $c^2$ ), and excluded  $m_{\tilde{\chi}_1^0}$  below  $m_{\tilde{\chi}_1^0} = 51$  GeV/ $c^2$  ( $m_{\tilde{\chi}_1^0} = 52$  GeV/ $c^2$ ) for  $m_{\tilde{t}_1} = 102$  GeV/ $c^2$  ( $m_{\tilde{t}_1} = 117$  GeV/ $c^2$ ). As the results from Run I have excluded almost all the stop mass below the kinematic cut off  $m_{\tilde{t}_1} = m_W + m_b + m_{\tilde{\chi}_1^0}$  for  $m_{\tilde{\chi}_1^0} < 40$  GeV/ $c^2$ , for this analysis we search for stop quark where the neutralino mass is  $m_{\tilde{\chi}_1^0} > 40$  GeV/ $c^2$ . In this search we use  $163 \pm 10$  pb $^{-1}$  [4] of  $p\bar{p}$  collision data at a center-of-mass energy of 1.96 TeV recorded by the Collider Detector at Fermilab (CDF) during the Tevatron Run II.

CDF is a general-purpose detector that is described in detail elsewhere [5]. The components relevant to this analysis are briefly described here. The charged-particle tracking system is closest to the beam pipe, and consists of multi-layer silicon detectors (SVX) [6] and a large open-cell drift chamber covering the pseudorapidity region  $|\eta| < 1$  [7]. The silicon detectors allow a precise measurement of a track's impact parameter with respect to the primary vertex in the plane transverse to the beam direction. The tracking system is enclosed in a superconducting solenoid, which in turn is surrounded by a calorimeter. The CDF calorimeter system is organized into electromagnetic and hadronic sections segmented in projective tower geometry, and covers the region  $|\eta| < 3.6$ . The electromagnetic calorimeters utilize a lead-scintillator sampling technique, whereas the hadron calorimeters use iron-scintillator technology. The central muon-detection system, used for this analysis, is located outside of the calorimeter and covers the range  $|\eta| < 1$ .

## II. DATA SAMPLE, EVENT SELECTION & BACKGROUNDS

In this analysis the  $\cancel{E}_T$  [7] is defined as the energy imbalance in the plane transverse to the beam direction. A jet is defined as a localized energy deposition in the calorimeter and is reconstructed using a cone algorithm with fixed radius  $\Delta R \equiv \sqrt{\Delta\eta^2 + \Delta\phi^2} = 0.4$  in  $\eta - \phi$  space [8]. We correct [8] jet  $E_T$  measurements and  $\cancel{E}_T$  for detector effects.

The data sample for this analysis was collected using an inclusive  $\cancel{E}_T$  trigger, which is distributed across three levels of online event selection. In the first and second levels of the trigger,  $\cancel{E}_T$  is required to be greater than 25 GeV and is calculated by summing over calorimeter trigger towers [9] with transverse energies above 1 GeV. At level-3  $\cancel{E}_T$  is required to be greater than 45 GeV and is recalculated using full calorimeter segmentation with a tower energy threshold of 100 MeV. We use events from the inclusive high- $p_T$  lepton ( $e$  or  $\mu$ ) samples to measure the trigger efficiency directly from data. To reduce systematic effects associated with the online trigger threshold, we select events offline with  $\cancel{E}_T > 55$  GeV, to be above the trigger threshold.

The event electromagnetic fraction ( $F_{em}$ ) and charged fraction ( $F_{ch}$ ) [10] are used to remove events associated with beam halo and cosmic ray sources. We reject events that contain little energy in the electromagnetic section of the calorimeter or that have mostly neutral-particle jets, by requiring  $F_{em} > 0.1$  and  $F_{ch} > 0.1$ .

The dominant backgrounds to the scalar top quark search in the jets and  $\cancel{E}_T$  signature are QCD multi-jet production,  $W$  and  $Z$  boson production in association with one or more jets, and top quark single and pair production. The ALPGEN generator [11] was used for the simulation of the  $W$  and  $Z$  boson plus parton production, with HERWIG [12] used to model parton showers. We use the exclusive  $Z \rightarrow ee + 1$  jet sample to determine a scale factor between data and simulation, and apply this factor to all  $W/Z$ +jets simulation samples. HERWIG was also used to estimate the contribution from single top quark and  $t\bar{t}$  production.

Data selection requirements were chosen to maximize the statistical significance of the scalar top quark signal over

background events based on studies of simulated event samples before the signal region data were examined. In addition to  $\cancel{E}_T > 55$  GeV, the signal region is defined by requiring that the two highest  $E_T$  jets ( $E_T^{j_1} > 35$  GeV,  $E_T^{j_2} > 25$  GeV) be in the central region ( $|\eta^{j_1}| < 1$ ,  $|\eta^{j_2}| < 1.5$ ). A third jet with  $E_T > 15$  GeV and  $|\eta| < 2.5$  is allowed, and we veto events with any additional jets with  $E_T > 10$  GeV and  $|\eta| < 3.6$ . To reject events with  $\cancel{E}_T$  resulting from jet energy mis-measurement, we require that the opening angle in the transverse plane between the two highest  $E_T$  jets satisfy  $\Delta\phi(j_1, j_2) < 165^\circ$ . The  $\cancel{E}_T$  direction must not be parallel to any of the jets. We require the minimum azimuthal separation between the direction of the jets and  $\cancel{E}_T$  of  $\min\Delta\phi(j, \cancel{E}_T) > 45^\circ$ . The  $\cancel{E}_T$  also must not be antiparallel to the first and second leading  $E_T$  jets:  $\Delta\phi(j_1, \cancel{E}_T) < 165^\circ$ ,  $\Delta\phi(j_2, \cancel{E}_T) < 150^\circ$ . These criteria reject most of the QCD multi-jet background events. To reduce the background contribution from  $W/Z$ +jets and top quark production, we reject events with one or more identified leptons with  $E_T > 10$  GeV (electron candidates) or  $p_T > 10$  GeV/ $c$  (muon candidates). Criteria similar to those in [13] are used to identify the leptons. To further reduce this background we require each jet not to be highly electromagnetic (jet electromagnetic fraction  $< 0.9$ ). The number of tracks associated to the first and second leading jets should be between 4 and 12 tracks. The lower cut is to reduce contributions from  $W$ +jets and  $Z$ +jets in which the gauge bosons decay into taus. The upper cut is to reduce the contributions from  $b$  jets that come from top quark decay. The first and second leading jets must also pass the cut  $\sum_i^{\text{tracks in jet}} dR_i > 0.15$ , where  $dR_i = \sqrt{(\phi_i - \phi_{jet})^2 + (\eta_i - \eta_{jet})^2}$ . This cut is to reduce the contributions

from  $W(\rightarrow \tau\nu)$ +jets where the hadronic  $\tau$  decay is mis-identified as a quark-jet. The number of tracks from hadronic tau decay is smaller compare to the tracks in the gluon and quark jets. Furthermore the tracks from hadronic tau decays are more collimated as compare to gluon and quark jets. A quantity which explores the correlation between the missing transverse energy and the transverse energy of the first and second leading jets,  $E_{T,12\text{MET}}^v$  [14], is required to be in the range  $-10 < E_{T,12\text{MET}}^v < 10$  GeV, to reduce contributions from QCD multi-jet and top quark production.

After applying these requirements, the data sample (pretag sample) contains 119 events. The total expected events from SM processes is  $105_{-11.2}^{+11.8}$ . The break down of the SM contributions is listed in Table I. The largest source of background in the pretag sample is the production of  $W$ +jets, where the  $W$  decays to a neutrino and an electron or muon that is not identified, or a tau which decays hadronically. In Figure 1 the  $\cancel{E}_T$  distribution of the pretag sample is compared with the predicted distribution from SM processes.

To estimate the QCD multi-jet contribution in the pretag sample, the selection requirement efficiency is measured as a function of  $\cancel{E}_T$  in an independent inclusive jet sample at low  $\cancel{E}_T$ . The extrapolated results of this measurement is then applied to the inclusive  $\cancel{E}_T$  sample after the  $W/Z$ +jets and top quark contributions have been subtracted.

The SVX information is used to tag heavy-flavor jets. We associate tracks to a jet by requiring that the track be within a cone of 0.4 in  $\eta - \phi$  space around the jet axis. We require the tracks to have  $P_T > 0.5$  GeV/ $c$ , positive impact parameter, and have a good SVX hit pattern. We take the sign of a track's impact parameter to be the sign of the scalar product of the impact parameter and the jet  $E_T$  vectors. We then define the impact parameter significance to be the impact parameter divided by its uncertainty. For tracks originating from the primary vertex the impact parameter significance distribution is symmetric around zero with a shape determined by the SVX resolution, while decay products of long lived objects tend to have large positive impact parameter significances. We use the negative impact parameter significance distribution to define the detector resolution function. For each track we determine the probability that the track comes from the primary vertex using this resolution function. We call this probability *track probability*. By construction, the *track probability* distribution is flat for tracks originating from the primary vertex, and peaks near zero for tracks from a secondary vertex. We combine the track probabilities for all tracks associated with a jet to form the *jet probability* ( $P_{\text{jet}}$ ) [15], the probability that all the tracks in the jet come from the primary vertex. The *jet probability* distribution is flat for jets originating from the primary vertex by construction, while for bottom and charm jets it peaks near zero.

We select events for the scalar top search by requiring one of the first two leading jets to be taggable and with a  $P_{\text{jet}} < 0.05$ . A taggable jet has at least two SVX tracks associated to it. If one of the two leading jets is tagged at  $P_{\text{jet}} < 0.05$ , and the other jet is taggable, this other jet is required to have  $P_{\text{jet}} < 0.45$ . The distribution of the minimum jet probability of the taggable jets in the pretag sample is shown in Figure 2. This requirement rejects approximately 92% of the background while its efficiency for the signal is about 30%.

### III. SIGNAL ACCEPTANCE AND SYSTEMATIC UNCERTAINTIES

The total detection efficiency ( $\epsilon_{\tilde{t}_1}$ ) for the scalar top quark signal is estimated using the PYTHIA event generator [16], and the CDF detector simulation program. The PYTHIA underlying event simulation was tuned to reproduce CDF data [17]. The samples were generated using the CTEQ5L [18] parton distribution functions (PDF), with the renormalization and factorization scales set to  $\mu = m_{\tilde{t}_1}$ . The total scalar top efficiency in the accessible mass region

vary from 0.02% to 2.1%. The efficiency increases for higher scalar top mass and larger mass difference between  $\tilde{t}_1$  and  $\tilde{\chi}_1^0$ .

The systematic uncertainty on the signal acceptance includes the uncertainties due to modeling gluon radiation from the initial-state or final-state partons (10%), and the choice of the PDF (2%). The limited size of the stop quark simulation samples gives a 5% statistical uncertainty. The signal acceptance uncertainty due to the jet energy scale varies from 6% to 33%, and the uncertainty on the luminosity is 6%. The uncertainty on the trigger efficiency is 2%. The systematic uncertainty for tagging heavy flavor jets is 10%.

#### IV. RESULTS

After applying heavy flavor tagging on the pretag data sample, we observe 11 events (tag sample), which is consistent with  $8.3_{-1.7}^{+2.3}$  events expected from SM processes. The break down of the SM contributions is listed in Table II. The largest source of background in the tag sample is the production of  $Z$ +jets, where the  $Z$  decays to two neutrinos. The QCD multi-jet contribution is estimated using the same method as for the pretag sample. In Figure 3 the  $\cancel{E}_T$  distribution of the tag sample is compared with the predicted distribution from SM processes. No evidence for scalar top production is observed. We calculate the upper limit at the 95% confidence level (C.L.) on the pair production cross section times the square of the branching ratio of the scalar top to a charm quark and a neutralino using a Bayesian approach [19] with a flat prior for the signal cross section and Gaussian priors for acceptance and background uncertainties. The upper limit on the cross section times branching ratio as function of the scalar top mass, for  $m_{\tilde{\chi}_1^0} = 40, 50, 55$  GeV/ $c^2$ , is shown in Figure 4 and is compared with the theoretical cross sections. The theoretical cross sections for scalar top quark production have been calculated at NLO using Prospino [20]. There are several reasons why the current analysis is not able to set a stop mass limit for  $m_{\tilde{\chi}_1^0} = 40$  GeV/ $c^2$  as compared to CDF Run I results. These are due to higher  $\cancel{E}_T$  trigger threshold in Run II, and larger systematic uncertainties in the jet energy scale and in the heavy flavor jet tagging in Run II, as compared to Run I.

In conclusion, we performed a search for scalar top in the jets and  $\cancel{E}_T$  topology using 163 pb $^{-1}$  of CDF Run II data. No evidence for scalar top is observed. We set an upper limit on the production cross section at the 95% C.L.

#### Acknowledgments

We thank the Fermilab staff and the technical staffs of the participating institutions for their vital contributions. This work was supported by the U.S. Department of Energy and National Science Foundation; the Italian Istituto Nazionale di Fisica Nucleare; the Ministry of Education, Culture, Sports, Science and Technology of Japan; the Natural Sciences and Engineering Research Council of Canada; the National Science Council of the Republic of China; the Swiss National Science Foundation; the A.P. Sloan Foundation; the Bundesministerium fuer Bildung und Forschung, Germany; the Korean Science and Engineering Foundation and the Korean Research Foundation; the Particle Physics and Astronomy Research Council and the Royal Society, UK; the Russian Foundation for Basic Research; the Comision Interministerial de Ciencia y Tecnologia, Spain; and in part by the European Community's Human Potential Programme under contract HPRN-CT-2002-00292, Probe for New Physics.

- 
- [1] H.P. Nilles, Phys. Rep. **110** (1984) 1;  
H.E. Haber and G.L. Kane, Phys. Rep. **117** (1985) 75.
  - [2] T. Affolder *et al.*, (CDF Collaboration), Phys. Rev. Lett. **84**, 5704 (2000).
  - [3] V.M. Abazov *et al.*, (DØ Collaboration), Phys. Rev. Lett. **93**, 011801 (2004).
  - [4] S. Klimentenko, J. Konigsberg and T. Liss, FERMILAB-FN-0741 (2003); D. Acosta *et al.*, Nucl. Instrum. Meth. **A494**, 57 (2002).
  - [5] CDF Collaboration, FERMILAB-PUB-96/390-E.
  - [6] A. Sill *et al.*, Nucl. Instrum. and Methods A **447**, 1 (2000).
  - [7] CDF uses a cylindrical coordinate system in which  $\theta$  is the polar angle to the proton beam,  $\phi$  is the azimuthal angle about the beam axis, and pseudorapidity is defined as  $\eta = -\ln \tan(\theta/2)$ . The transverse energy and transverse momentum are defined as  $E_T = E \sin\theta$  and  $p_T = p \sin\theta$ , where  $E$  is energy measured in the calorimeter and  $p$  is momentum measured by the tracking system. The missing transverse energy vector,  $\cancel{E}_T$ , is  $-\sum_i E_T^i \mathbf{n}_i$ , where  $\mathbf{n}_i$  is the unit vector in the azimuthal plane that points from the beamline to the  $i$ th calorimeter tower.
  - [8] T. Affolder *et al.* (CDF Collaboration), Phys. Rev. **D64**, 032001 (2001).

- [9] The physical calorimeter towers are organized into larger trigger towers, covering approximately 0.26 in  $\Delta\phi$  and 0.22 in  $\Delta\eta$ .
- [10]  $F_{em}$  is the ratio of the energy measured by the electromagnetic calorimeter to the total energy contained in jets of cone radius  $\Delta R = 0.4$  with  $E_T > 10$  GeV and  $|\eta| < 3.6$ .  $F_{ch}$  is the fraction of the jet energy carried by measured charged-particle tracks ( $p_T > 0.5$  GeV/c) averaged over the central jets with  $|\eta| < 0.9$ . These variables are similar to ones used in T. Affolder *et al.* (CDF Collaboration), Phys. Rev. Lett. **88**, 041801 (2002).
- [11] M.L. Mangano *et al.*, JHEP **07**, 001 (2003). We use version 1.2.
- [12] G. Corcella *et al.*, JHEP **01**, 010 (2001); hep-ph/0210213. We use version 6.4a.
- [13] D. Acosta *et al.* (CDF Collaboration), FERMILAB-PUB-04/051-E., accepted by Phys. Rev. Lett.
- [14] The quantity  $E_{T_{J12MET}}^v$  is defined as follow :  $\vec{E}_{T_{J12MET}} = \vec{E}_{T_{J1}} + \vec{E}_{T_{J2}} + M\vec{E}T$  ( $\vec{E}_{T_{J1}}$  and  $\vec{E}_{T_{J2}}$  are, respectively, the vector of the transverse energy of the first and second leading jets, and  $M\vec{E}T$  is the vector of the missing transverse energy),  $\vec{E}_{T_{J12}} = \vec{E}_{T_{J1}} + \vec{E}_{T_{J2}}$ ,  $\vec{v} = \vec{E}_{T_{J12}} / |\vec{E}_{T_{J12}}|$ ,  $E_{T_{J12MET}}^v = \vec{E}_{T_{J12MET}} \cdot \vec{v}$ .
- [15] F. Abe *et al.* (CDF Collaboration), Phys. Rev. D **53**, 1051 (1996).
- [16] T. Sjostrand, P. Eden, C. Friberg, L. Lonnblad, G. Miu, S. Mrenna and E. Norrbin, Computer Physics Commun. 135, 238 (2001), version 6.203.
- [17] T. Affolder *et al.* (CDF Collaboration), Phys. Rev. D **65** 092002 (2002).
- [18] H. L. Lai *et al.* (CTEQ Collaboration), Eur. Phys. J. **C12** 375 (2000).
- [19] J. Conway, CERN 2000-005, 247 (2000). The posterior probability density is rendered normalizable by introducing a reasonably large cutoff.
- [20] W. Beenakker *et al.*, Phys. Rev. Lett. **83**, 3780 (1999);  
T. Plehn <http://pheno.physics.wisc.edu/~plehn/prospino/prospino.html>.

TABLE I: The number of expected events from various SM sources in the scalar top signal region (before applying heavy flavor jet tagging). The first uncertainty is from the limited simulation statistics and the second is from the various systematics.

Source	Events expected
$W(\rightarrow e\nu) + 2$ jets	$5.71 \pm 1.30 \pm 0.68$
$W(\rightarrow \mu\nu) + 2$ jets	$24.7 \pm 2.3 \pm 2.9$
$W(\rightarrow \tau\nu) + 2$ jets	$23.0 \pm 2.1 \pm 2.7$
$Z(\rightarrow \mu\mu) + 2$ jets	$1.12 \pm 0.14 \pm 0.13$
$Z(\rightarrow \tau\tau) + 2$ jets	$5.69 \pm 0.10 \pm 0.07$
$Z(\rightarrow \nu\nu) + 2$ jets	$39.5 \pm 2.7 \pm 4.7$
$WW$	$1.99 \pm 0.19 \pm 0.31$
$WZ$	$0.95 \pm 0.11 \pm 0.15$
$ZZ$	$0.75 \pm 0.06 \pm 0.12$
$t\bar{t}$	$1.23 \pm 0.15 \pm 0.12$
<i>single top(s - channel)</i>	$0.49 \pm 0.03 \pm 0.07$
<i>single top(t - channel)</i>	$0.42 \pm 0.04 \pm 0.06$
QCD	$5.05^{+3.72}_{-1.09}$ (total)
Total Events	$105^{+11.8}_{-11.2}$ (total)
Data	119

TABLE II: The number of expected events from various SM sources in the scalar top signal region (after applying heavy flavor jet tagging). The first uncertainty is from the limited simulation statistics and the second is from the various systematics.

Source	Events expected
$W(\rightarrow e\nu) + 2$ jets	$0.027 \pm 0.012 \pm 0.0048$
$W(\rightarrow \mu\nu) + 2$ jets	$0.90 \pm 0.36 \pm 0.16$
$W(\rightarrow \tau\nu) + 2$ jets	$2.08 \pm 0.55 \pm 0.37$
$Z(\rightarrow \mu\mu) + 2$ jets	$0.043 \pm 0.025 \pm 0.026$
$Z(\rightarrow \tau\tau) + 2$ jets	$0.045 \pm 0.026 \pm 0.027$
$Z(\rightarrow \nu\nu) + 2$ jets	$2.7 \pm 0.63 \pm 0.79$
$WW$	$0.19 \pm 0.052 \pm 0.038$
$WZ$	$0.19 \pm 0.044 \pm 0.038$
$ZZ$	$0.19 \pm 0.027 \pm 0.038$
$t\bar{t}$	$0.68 \pm 0.10 \pm 0.15$
<i>single top(s - channel)</i>	$0.36 \pm 0.024 \pm 0.074$
<i>single top(t - channel)</i>	$0.12 \pm 0.019 \pm 0.030$
QCD	$0.84^{+1.7}_{-0.8}$ (total)
Total Events	$8.3^{+2.3}_{-1.7}$ (total)
Data	11

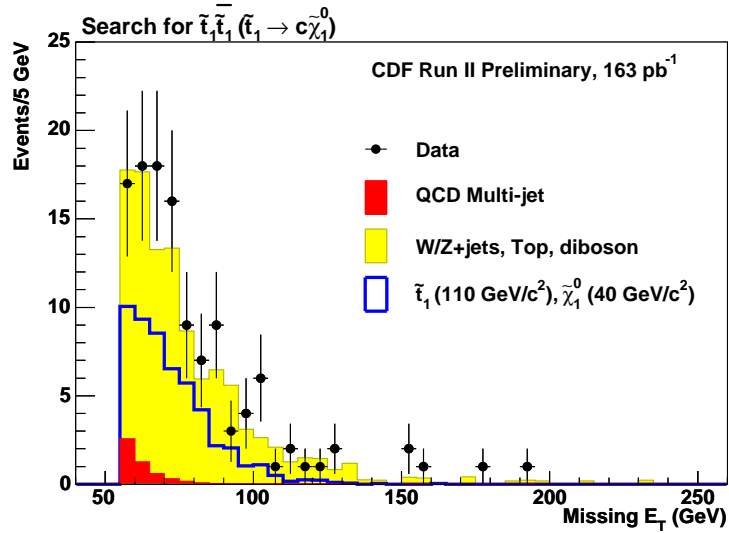


FIG. 1: The  $\cancel{E}_T$  distribution of the pretag sample is compared with the predicted distribution from SM processes. Also shown is the expected distribution arising from scalar top quark production and decay with  $m_{\tilde{t}_1} = 110 \text{ GeV}/c^2$  and  $m_{\tilde{\chi}_1^0} = 40 \text{ GeV}/c^2$ .

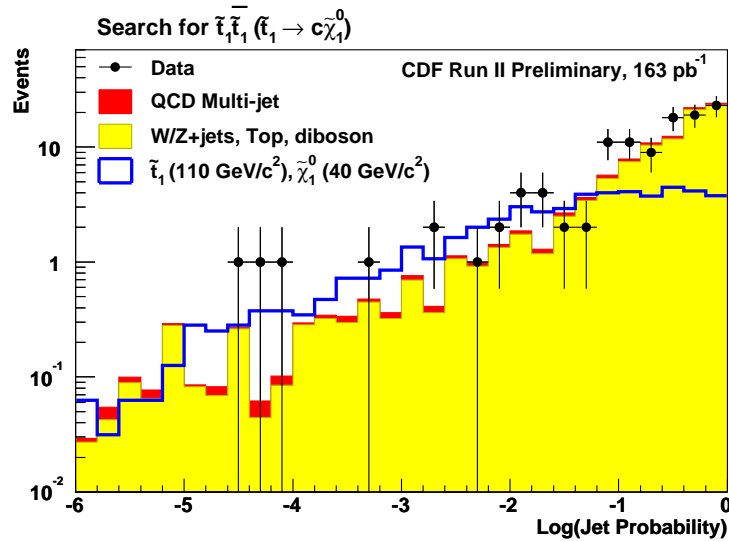


FIG. 2: The distribution of the minimum jet probability of the taggable jets in the pretag sample. Also shown is the expected distribution arising from scalar top quark production and decay with  $m_{\tilde{t}_1} = 110 \text{ GeV}/c^2$  and  $m_{\tilde{\chi}_1^0} = 40 \text{ GeV}/c^2$ .

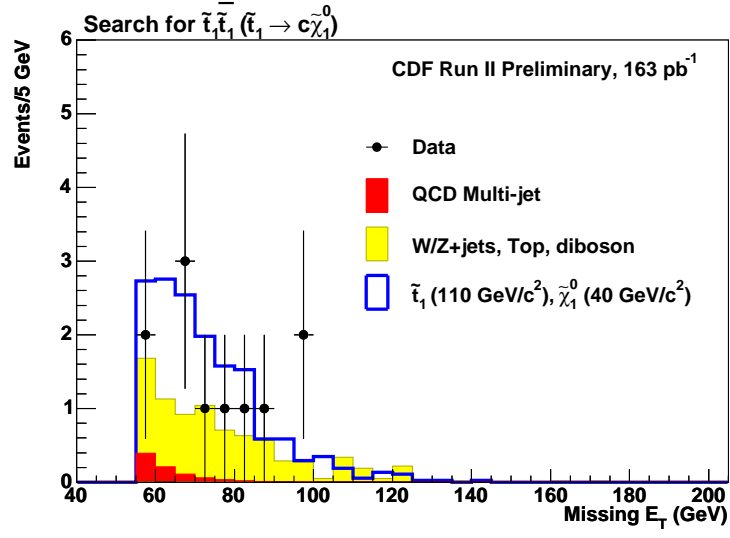


FIG. 3: The  $\cancel{E}_T$  distribution of the tag sample is compared with the predicted distribution from SM processes. Also shown is the expected distribution arising from scalar top quark production and decay with  $m_{\tilde{t}_1} = 110 \text{ GeV}/c^2$  and  $m_{\tilde{\chi}_1^0} = 40 \text{ GeV}/c^2$ .

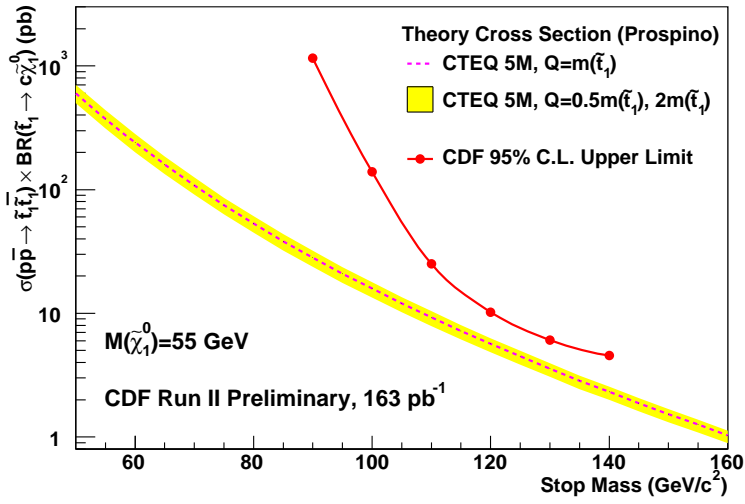
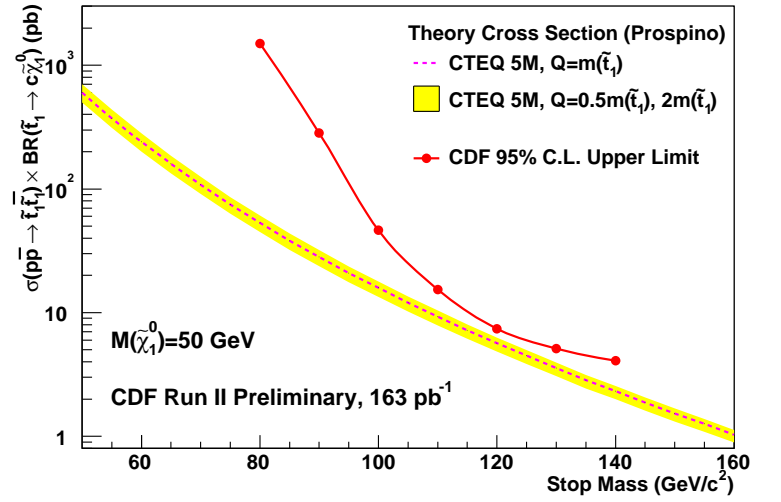
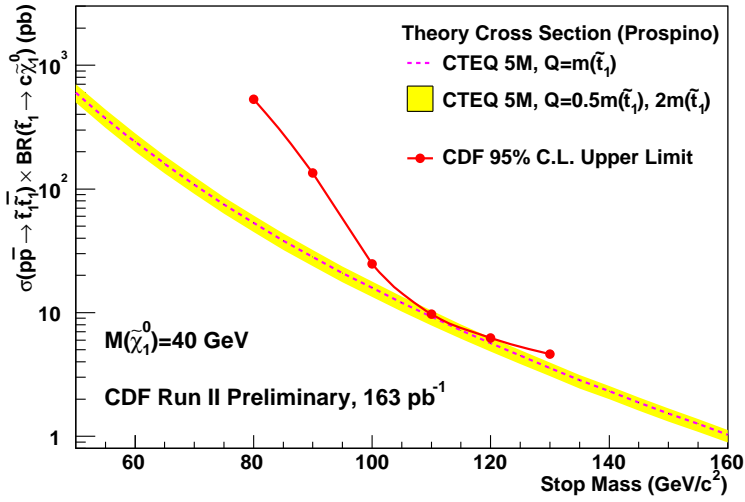


FIG. 4: The 95% CL upper limit on the cross section for pair production of scalar top quarks. These limits curves are for  $M(\tilde{\chi}_1^0) = 40, 50, 55 \text{ GeV}/c^2$ .